TECHNOMETRICS
https://doi.org/10.1080/00401706.2018.1512900

Taylor & Francis
Taylor & Francis Group

Bayesian Analysis of Accumulated Damage Models in Lumber Reliability

Chun-Hao Yang[a], James V. Zidek[b], and Samuel W. K. Wong[a,c]

[a]Department of Statistics, University of Florida, Gainesville, FL; [b]Department of Statistics, University of British Columbia, Vancouver, Canada; [c]Department of Statistics and Actuarial Science, University of Waterloo, Waterloo, Canada

ABSTRACT

Wood products that are subjected to sustained stress over a period of long duration may weaken, and this effect must be considered in models for the long-term reliability of lumber. The damage accumulation approach has been widely used for this purpose to set engineering standards. In this article, we revisit an accumulated damage model and propose a Bayesian framework for analysis. For parameter estimation and uncertainty quantification, we adopt approximation Bayesian computation (ABC) techniques to handle the complexities of the model. We demonstrate the effectiveness of our approach using both simulated and real data, and apply our fitted model to analyze long-term lumber reliability under a stochastic live loading scenario. Code is available at *https://github.com/wongswk/abc-adm*.

ARTICLE HISTORY
Received May 2017
Revised July 2018

KEYWORDS
Approximate Bayesian computation; Duration of load; Failure time distribution

1. Introduction

The long-term reliability of lumber is an important consideration in the construction of wood-based structures. That led Foschi (1979) to advance the development of a system for setting lumber standards with an explicit role for probability models and return periods, and other key concepts in the theory of reliability. There are challenges associated with the application of structural reliability to wood products, as lumber has considerable inherent variability and is susceptible to the "duration of load (DOL)" effect. The DOL effect was first studied empirically by Wood (1951). Briefly, when a piece of lumber is subject to a sustained stress over a period of long duration, the stress may cause it to first deform (known as *creep*) and then eventually to fail (known as *creep rupture*). Thus for structural engineering applications, the DOL effect has to be taken into consideration when calculating safety factors, that is, to ensure a safe load-carrying capacity for the structure. Foschi, Folz, and Yao (1989) conducted an in-depth study of this nature and presented the reliability assessment results for structural usage of lumber, where the stress on an individual piece may be a combination of random (e.g., from snow or owner occupancy) and constant (e.g., from the dead weight of structure) loadings over time.

The time to failure of lumber products with a long intended life span (e.g., 30 or more years) cannot be measured for practical reasons, so instead various accelerated testing methods have been developed to study the DOL effect (Barrett and Foschi 1978). These tests are described in terms of the load applied over time $\tau(t), t \geq 0$. Two such commonly used loading patterns are the *ramp load* and *constant load*. For a ramp load test, the load is applied at a linearly increasing rate $\tau(t) = kt$ until the piece breaks, where k is the selected loading rate in *psi* (pounds per square inch) per unit of time. One particular ramp loading rate k_s is set for calibration purposes, corresponding to the way the short-term strength of the piece τ_s is defined: letting random variable T_s denote the breaking time of the piece when ramp load rate k_s is used, then $\tau_s \equiv k_s T_s$. In contrast, the constant load test is based on applying a constant load τ_c over time: the procedure begins with an initial ramp loading phase that increases the load to the preset level τ_c, after which the test continues under that constant load. The test ends when either the piece breaks, or the piece has survived a specified time period without breaking. For practical purposes, the time period after which a constant load test is truncated is usually a few months to a few years.

To model the DOL effect and project the results obtained from accelerated tests to longer time periods, the damage accumulation approach has received substantial attention (e.g., Foschi and Yao 1986; Gerhards and Link 1987; Rosowsky and Ellingwood 1992; Hoffmeyer and Sørensen 2007; Svensson 2009). In this context, $\alpha(t)$ denotes the damage state of the piece as a function of time, such that $\alpha = 0$ indicates no damage and $\alpha = 1$ indicates failure. While $\alpha(t)$ is generally a latent function and not directly measurable—as we only observe $\alpha(0) = 0$ and $\alpha(T) = 1$ where T is the piece-specific random failure time—the construction of theoretical models for $\alpha(t)$ has nonetheless served as a useful device for fitting experimental data. A key feature of these models is that they provide a corresponding theoretical damage accumulation curve $\alpha(t)$ for any input loading profile $\tau(t)$ desired.

Accumulated damage models (ADMs) express the rate of damage accumulation in terms of a differential equation that involves $\tau(t)$ and τ_s. Various functional forms of ADMs have been proposed. For example, the "US model" was introduced by Gerhards (1979) and slightly modified by Zhai (2011), which specifies

$$\frac{d}{dt}\alpha(t)\mu = \exp\left(-A + B\frac{\tau(t)}{\tau_s}\right),$$

CONTACT Samuel W. K. Wong *samuel.wong@uwaterloo.ca* M3 3104, Department of Statistics and Actuarial Science, University of Waterloo, Waterloo, ON N2L 3G1, Canada.

where A and B are random effects for each specific piece of lumber, and μ is a constant with units "time" to ensure dimensional consistency since the right-hand side is unitless. The "Canadian model" was introduced by Foschi and Yao (1986), and we consider the modified version with a reparameterization based on dimensional analysis to ensure dimensional consistency (Wong and Zidek 2018), given by

$$\frac{d}{dt}\alpha(t)\mu = [(a\tau_s)(\tau(t)/\tau_s - \sigma_0)_+]^b + [(c\tau_s)(\tau(t)/\tau_s - \sigma_0)_+]^n \alpha(t), \quad (1)$$

where a, b, c, n, σ_0 are piece-specific random effects and $(x)_+ = \max(x, 0)$. Here, σ_0 serves as the stress ratio threshold in that damage starts to accumulate only when $\tau(t)/\tau_s > \sigma_0$. The Canadian model was previously shown to provide a good fit to experimental data in Foschi, Folz, and Yao (1989); since its introduction, that model has also been considered in subsequent damage modeling research (e.g., Fridley, Tang, and Soltis 1992; Sørensen and Svensson 2005; Li and Lam 2016). Hence the Canadian model, as parameterized in Equation (1), will be the main focus of this article, and to facilitate comparability with Foschi's results we set $\mu = 1$ hour and use "hours" as our time unit.

Previous work by Foschi and Yao (1986) and Gerhards and Link (1987) have proposed nonlinear least squares (NLS) and regression-based methods to estimate the parameters in these models based on constant load experimental data. The fitted models were then applied with various stochastic loadings $\tau(t)$ to simulate real conditions such as snow loads and occupancy loads, to assess the reliability of pieces over long periods of time. Thus, the estimated ADM parameters have played a crucial role in the development of safety factors for wood-based structures. However, due to computational complexities, appropriate statistical methods of parameter estimation have not been previously attempted for these models. Such methods are necessary to better quantify the effect of uncertainty in parameter estimates on reliability. The advances in modern statistical computation motivate us to revisit this problem and develop the necessary foundations on which current engineering standards can be evaluated and improved. We adopt a Bayesian approach for inference, as it provides a coherent way to account for parameter uncertainties in the posterior distribution for future time to failure, and to incorporate any prior knowledge in the analysis.

The key application of this article is to assess long-term lumber reliability under stochastic loadings. Using the fitted models, we may estimate the probability of failure within a certain period when lumber is placed in service under various loading scenarios, for example, the probability that an individual piece will break within 30 years under loads typical of residential dwelling units. The probabilities of failure are used to compute reliability indices, and our Bayesian approach readily enables the construction of posterior intervals for these reliabilities as well.

The remainder of the article is laid out as follows. In Section 2, we discuss the difficulties encountered in parameter estimation for ADMs, and propose an adaptation of the approximate Bayesian computation (ABC) technique to tackle this problem. In Section 3, we present results of our estimation procedure on simulated data to assess its effectiveness. Analysis of a real dataset is provided in Section 4. In Section 5, we review how the ADMs are used for time-to-failure prediction under a live loading scenario, and apply our fitted model for that purpose. We conclude the article with a brief discussion in Section 6.

2. Parameter Estimation for the Canadian ADM

The parameter estimation problem of primary interest here is the scenario where a random sample of pieces is subject to the load profile

$$\tau(t) = \begin{cases} kt, & \text{for } t \le T_0 \\ \tau_c, & \text{for } t > T_0 \end{cases}, \quad (2)$$

where τ_c is the selected constant-load level, and $T_0 = \tau_c/k$ is the time required for the load to reach τ_c under the ramp-loading rate k. For calibration purposes, the test is run with $k = k_s$ to match the ramp-loading rate used to define the short-term strength of a piece of lumber (see Introduction). The load profile in Equation (2) is the general constant-load test, and includes the ramp-load test as a special case which is obtained by setting $\tau_c = +\infty$. We first construct the likelihood function of the model parameters based on the observed data $\boldsymbol{t}_{\text{obs}}$ for the failure times in the sample.

When we set $k = k_s$ and $\tau_c = +\infty$ for a ramp-load test, T_s can be determined as a function of the piece-specific random effects. For the Canadian ADM (1), T_s can only be solved numerically; it can be shown that T_s is determined by the solution to the equation (see Appendices)

$$H(T_s) = \frac{(akT_s)^b}{(ckT_s)^{n(b+1)/(n+1)}} \left(\frac{\mu(n+1)}{T_s}\right)^{\frac{b-n}{n+1}} \times \int_0^{-\log H(T_s)} e^{-u} u^{(b+1)/(n+1)-1} du, \quad (3)$$

where

$$H(t) = \exp\left\{-\frac{1}{\mu}(ckT_s)^n \frac{T_s}{n+1}\left(\frac{t}{T_s} - \sigma_0\right)^{n+1}\right\}.$$

This provides an implicit solution of T_s as a function of a, b, c, n, σ_0.

The constant-load test with the same ramp-loading rate $k = k_s$ for the initial portion ($t \le T_0$) then has a failure time T_c that can be expressed in terms of T_s and the piece-specific random effects,

$$T_c = -\frac{1}{C_2}\log\left(\frac{\frac{C_1}{C_2}H^\star(T_0) + C_3}{1 + \frac{C_1}{C_2}}\right),$$

where

$$C_1 = \frac{1}{\mu}\left[akT_s\left(\frac{T_0}{T_s} - \sigma_0\right)\right]^b$$
$$C_2 = \frac{1}{\mu}\left[ckT_s\left(\frac{T_0}{T_s} - \sigma_0\right)\right]^n$$
$$C_3 = \alpha(T_0)H^\star(T_0)$$
$$H^\star(T_0) = \exp\{-C_2 T_0\}$$
$$\alpha(T_0) = \frac{1}{H(T_0)}\frac{(akT_s)^b}{(ckT_s)^{n(b+1)/(n+1)}}\left(\frac{\mu(n+1)}{T_s}\right)^{\frac{b-n}{n+1}} \times \int_0^{-\log H(T_0)} e^{-u} u^{(b+1)/(n+1)-1} du.$$

Thus, the complete solution for the constant-load failure time T is

$$T = \begin{cases} T_s & \text{if } T_s \le T_0 \\ T_c & \text{if } T_s > T_0 \end{cases}. \tag{4}$$

To model piece-to-piece variation, it is customary to assign distributions to the piece-specific random effects a, b, c, n, σ_0. For this purpose, independent log-Normals were used in Foschi, Folz, and Yao (1989) which satisfy the basic condition that each of the random effects is positive-valued. We take the same approach in this article to facilitate comparability of results; further discussion concerning these random effects is provided in Section 6. The random effects distributions are thus specified as follows in our application:

$$\begin{aligned} a|\mu_a, \sigma_a &\sim \text{Log-Normal}(\mu_a, \sigma_a) \\ b|\mu_b, \sigma_b &\sim \text{Log-Normal}(\mu_b, \sigma_b) \\ c|\mu_c, \sigma_c &\sim \text{Log-Normal}(\mu_c, \sigma_c) \\ n|\mu_n, \sigma_n &\sim \text{Log-Normal}(\mu_n, \sigma_n) \\ \eta|\mu_{\sigma_0}, \sigma_{\sigma_0} &\sim \text{Log-Normal}(\mu_{\sigma_0}, \sigma_{\sigma_0}) \text{ and set } \sigma_0 = \frac{\eta}{1+\eta}. \end{aligned} \tag{5}$$

Therefore, the parameter vector of interest is $\theta = (\mu_a, \sigma_a, \mu_b, \sigma_b, \mu_c, \sigma_c, \mu_n, \sigma_n, \mu_{\sigma_0}, \sigma_{\sigma_0})$.

The likelihood contribution of one observation $T = t$ would be

$$\begin{aligned} f_T(t|\theta) &= \int \cdots \int p(t|a, b, c, n, \sigma_0) \\ &\quad \times p(a, b, c, n, \sigma_0|\theta) da\, db\, dc\, dn\, d\sigma_0 \\ &= \int \cdots \int I_{\{(a,b,c,n,\sigma_0):h(a,b,c,n,\sigma_0)=t\}}(a, b, c, n, \sigma_0) \\ &\quad \times p(a, b, c, n, \sigma_0|\theta)\, da\, db\, dc\, dn\, d\sigma_0, \end{aligned}$$

where h is the implicit solution of T expressed in terms of a, b, c, n, σ_0 and $I_{\{\cdot\}}(\cdot)$ is the indicator function (i.e., $I_A(x) = 1$ if $x \in A$ and $I_A(x) = 0$ if $x \notin A$). The set $\{(a, b, c, n, \sigma_0) : h(a, b, c, n, \sigma_0) = t\}$ involves h which has no closed form. Therefore in practice one cannot directly calculate the likelihood using this integral.

In addition, the constant-load test is truncated after a certain period of time for practical reasons, so the likelihood of the observed data t_{obs} for one board would be

$$f(t_{\text{obs}}|\theta) = f_T(t_{\text{obs}}|\theta) I_{\{t:t\le t_c\}}(t) + (1 - F_T(t_c|\theta))\, I_{\{t:t>t_c\}}(t), \tag{6}$$

where t_c is the censoring time and $f_T(\cdot|\theta)$ and $F_T(\cdot|\theta)$ are, respectively, the density function and the distribution function of T determined by the solution (4). Since $f_T(t|\theta)$ is intractable, so is the likelihood $f(t_{\text{obs}}|\theta)$.

It can be seen that the form of $f_T(t|\theta)$ resembles that of a nonlinear random-effects model, with the failure time of the ith board in a random sample modeled as $T_i = h(a_i, b_i, c_i, n_i, \sigma_{0,i})$. However, there are two important distinguishing features of the ADM. First, there is no explicit error term ϵ_i. This follows from the fundamental modeling assumption of ADMs seen in the Introduction: given the realizations of the random effects, the damage accumulation is described by a deterministic ODE. Second, the function h has no analytic form. Thus, existing approaches for estimation of nonlinear mixed-effects models (e.g., Pinheiro and Bates 1995; Bae and Kvam 2004) are not readily applicable here.

For a given parameter vector θ, the likelihood can be computed numerically with brute-force to achieve any required level of approximation accuracy. We may simulate a large number of T's using (4) to approximate its probability density, for example, using kernel density estimation. This poses no conceptual difficulty since it is simple to generate a, b, c, n, σ_0 from (5) and then with these random effects, we can solve for T using (4) numerically. However, a parameter estimation procedure, if we wish to maximize the likelihood, will require many probability density evaluations, which makes this approach impractical. Also, analytical gradient-based or convex optimization methods cannot be used with this likelihood function.

The estimated parameters will finally be used in the context of constructing time-to-failure distributions under simulated live loadings. To propagate uncertainty in the parameter estimates to those distributions in a statistically coherent way, we adopt a Bayesian approach for inference on θ based on Markov chain Monte Carlo (MCMC) simulation. MCMC is also an appealing approach for exploring the parameter space without requiring gradients. Nevertheless, a vanilla MCMC algorithm also requires repeated likelihood computation at each iteration. In what follows, we adopt the approximate Bayesian computation (ABC) technique as a likelihood-free version of MCMC, which only requires the ability to generate data from the model; thus, this allows us to sample θ in an efficient way. In Section 2.1, we briefly review ABC as based on the MCMC algorithm described in Fearnhead and Prangle (2012). In Section 2.2, we propose suitable modifications to the algorithm to handle the censoring in our data. Some implementation details are provided in Section 2.3.

2.1 Review of ABC-MCMC

Let θ be the parameter vector of interest and $\boldsymbol{y}_{\text{obs}}$ be the n-dimensional observed data. The key step in ABC is the approximation of the posterior

$$\pi(\theta|\boldsymbol{y}_{\text{obs}}) \approx \pi_{\text{ABC}}(\theta|\boldsymbol{s}_{\text{obs}}) \propto \pi(\theta) p(\boldsymbol{s}_{\text{obs}}|\theta),$$

where $\boldsymbol{s}_{\text{obs}} = S(\boldsymbol{y}_{\text{obs}})$ for some summary statistics $S(\cdot)$. Then $p(\boldsymbol{s}_{\text{obs}}|\theta)$ is defined via a further approximation step,

$$p(\boldsymbol{s}_{\text{obs}}|\theta) = \int \pi(\boldsymbol{y}|\theta) K_\delta(S(\boldsymbol{y}) - s_{\text{obs}}) d\boldsymbol{y},$$

where $K_\delta(\cdot)$ is a density kernel with bandwidth $\delta > 0$ (Fearnhead and Prangle 2012). Hence, an MCMC sampling algorithm for this ABC posterior is given in Algorithm 1, where g is a specified proposal distribution.

2.2 Modified ABC-MCMC for Censored Data

From previous research (e.g., Beaumont, Zhang, and Balding 2002; Joyce et al. 2008; Fearnhead and Prangle 2012), the choice of summary statistics plays a crucial role in the success of an ABC algorithm. Ideally, if the summary statistics $S(\cdot)$ are sufficient for θ, then the ABC posterior is identical to the true posterior. For most real applications it is impossible to find such a sufficient statistic, and so $S(\cdot)$ would be chosen to contain as much

Algorithm 1: ABC-MCMC sampling algorithm of Fearnhead and Prangle (2012)

1. Generate θ' from $g(\theta|\theta_k)$
2. Generate $\boldsymbol{y}$ from $f(\boldsymbol{y}|\theta')$ and find $\boldsymbol{s} = S(\boldsymbol{y})$
3. Calculate
$$\alpha(\theta', \theta_k) = \min\left(1, \frac{K_\delta(\boldsymbol{s} - \boldsymbol{s}_{obs})\pi(\theta')g(\theta'|\theta_k)}{K_\delta(\boldsymbol{s}_k - \boldsymbol{s}_{obs})\pi(\theta_k)g(\theta_k|\theta')}\right)$$
4. Accept θ' and $\boldsymbol{s}$ with probability $\alpha(\theta', \theta_k)$; otherwise $\theta_{k+1} = \theta_k$ and $\boldsymbol{s}_{k+1} = \boldsymbol{s}_k$

information about θ as possible while being of fairly low dimension. In our model, the number (or proportion) of censored observations is certainly an informative statistic, but on a different scale than other summary statistics such as means or quantiles. This problem could potentially be solved by designing an appropriate metric that combines statistics computed from the censored and uncensored observations. But here we can instead exploit the censoring in our context and factorize the likelihood such that the density kernel approximation is only applied to the uncensored observations instead of the whole dataset.

Based on the likelihood (6), the joint likelihood of the n-dimensional observation $\boldsymbol{t}_{\text{obs}}$ of an independent and identically distributed (iid) sample is

$$\begin{aligned} f(\boldsymbol{t}_{\text{obs}}|\theta) &= f_T(\boldsymbol{t}'_{\text{obs}}|\theta)\,[1 - F_T(t_c|\theta)]^{n_c} \\ &= \left[\prod_{i=1}^{n-n_c} f_T(t'_{\text{obs},i}|\theta)\right][1 - F_T(t_c|\theta)]^{n_c} \\ &= \left[\prod_{i=1}^{n-n_c} \frac{f_T(t'_{\text{obs},i}|\theta)}{F_T(t_c|\theta)}\right][F_T(t_c|\theta)]^{n-n_c}\,[1 - F_T(t_c|\theta)]^{n_c}, \end{aligned} \tag{7}$$

where by exchangeability n_c is the number of censored pieces in the observed data and $\boldsymbol{t}'_{\text{obs}}$ is the uncensored part of the observed data. Since $\frac{f_T(t|\theta)}{F_T(t_c|\theta)}, 0 \le t \le t_c$ is a normalized density, the density kernel approximation when applied to $\prod_{i=1}^{n-n_c} \frac{f_T(t'_{\text{obs},i}|\theta)}{F_T(t_c|\theta)}$ will have correct scaling for any choice of summary statistics on $\boldsymbol{t}'_{\text{obs}}$. This yields the posterior

$$\begin{aligned} \pi(\theta|\boldsymbol{t}_{\text{obs}}) &\propto f(\boldsymbol{t}_{\text{obs}}|\theta)\pi(\theta) \\ &= \left[\prod_{i=1}^{n-n_c} \frac{f_T(t'_{\text{obs},i}|\theta)}{F_T(t_c|\theta)}\right][F_T(t_c|\theta)]^{n-n_c} \\ &\quad \times [1 - F_T(t_c|\theta)]^{n_c}\pi(\theta) \\ &\propto \pi(\theta|\boldsymbol{t}'_{\text{obs}})\,[F_T(t_c|\theta)]^{n-n_c}\,[1 - F_T(t_c|\theta)]^{n_c} \\ &\approx \pi_{\text{ABC}}(\theta|\boldsymbol{s}'_{\text{obs}})\,[F_T(t_c|\theta)]^{n-n_c}\,[1 - F_T(t_c|\theta)]^{n_c}, \end{aligned}$$

where $\boldsymbol{s}'_{\text{obs}} = S(\boldsymbol{t}'_{\text{obs}})$, and $F_T(t_c|\theta)$ can be estimated consistently by $\hat{F}_T(t_c|\theta) = n^{-1}\sum_{i=1}^{n} I_{\{t_i:t_i<t_c\}}(t_i)$ using the simulated t_i from $f_T(t|\theta)$ that will already be generated as part of an ABC-MCMC algorithm.

This provides an approximation of the Metropolis–Hastings (M-H) acceptance ratio. We present Algorithm 2, as a version of Algorithm 1 generalized to handle censoring, which we use throughout this article.

Algorithm 2: ABC-MCMC sampling algorithm for censored data

1. Generate θ' from $g(\theta|\theta_k)$
2. Generate $\boldsymbol{t} = (t_1, \ldots, t_n)$ from $f_T(t|\theta')$ and truncate the data with the censoring level t_c
3. Calculate $\boldsymbol{s} = S(\boldsymbol{t}')$ and the censored proportion $\hat{p}_{t_c} = n^{-1}\sum_{i=1}^{n} I_{\{t_i:t_i<t_c\}}(t_i)$ where $\boldsymbol{t}'$ is the uncensored part of the simulated data
4. Calculate
$$\begin{aligned} \alpha(\theta', \theta_k) = \min\Bigg(1, &\frac{K_\delta(\boldsymbol{s} - \boldsymbol{s}'_{obs})\pi(\theta')g(\theta'|\theta_k)}{K_\delta(\boldsymbol{s}_k - \boldsymbol{s}'_{obs})\pi(\theta_k)g(\theta_k|\theta')} \\ &\times \left(\frac{1 - \hat{p}_{t_c}}{1 - \hat{p}_{t_c,k}}\right)^{n-n_c}\left(\frac{\hat{p}_{t_c}}{\hat{p}_{t_c,k}}\right)^{n_c}\Bigg) \end{aligned}$$
5. Accept $(\theta', \boldsymbol{s}, \hat{p}_{t_c})$ with probability $\alpha(\theta', \theta_k)$; otherwise $(\theta_{k+1}, \boldsymbol{s}_{k+1}, \hat{p}_{t_c,k+1}) = (\theta_k, \boldsymbol{s}_k, \hat{p}_{t_c,k})$

2.3 Choice of Summary Statistics, Kernel, and Bandwidth δ

To implement Algorithm 2, we need to first choose the summary statistic $S(\cdot)$, the kernel function $K(\cdot)$, and the bandwidth δ. For our model, there is clearly no natural sufficient statistic for θ. Hence, for implementation we choose 19 equally spaced quantiles from 5% to 95% as the summary statistics for the uncensored part and a Normal kernel; the use of quantiles as summary statistics was previously suggested in Allingham, King, and Mengersen (2009). To determine the bandwidth δ, we run several short simulations with different values of δ and choose the smallest one that attains a 1% acceptance rate as suggested by Fearnhead and Prangle (2012).

3. Simulated Examples

In this section, we set up simulation studies to illustrate the proposed Algorithm 2. First, we choose the following fairly diffuse prior distributions for most of the parameters in θ, which will be used for both the simulated examples as well as the following real data analysis,

$$\begin{aligned} \mu_a, \mu_b, \mu_c, \mu_n &\overset{\text{iid}}{\sim} N(0, 20) \\ \sigma_a^2, \sigma_b^2, \sigma_c^2, \sigma_n^2, \sigma_{\sigma_0}^2 &\overset{\text{iid}}{\sim} \text{Inv-Gamma}(0.01, 0.01). \end{aligned}$$

The exception is μ_{σ_0}, for which we set the more informative prior $\mu_{\sigma_0} \sim N(0, 1)$ to correspond with the a priori belief that on average no damage accumulates on a piece of lumber until the stress level exceeds 50% of its short-term strength τ_s (Smith, Landis, and Gong 2003, p. 181).

The two simulation scenarios we demonstrate here are (i) fitting one constant-load dataset, and (ii) fitting two datasets with different constant-load levels simultaneously. The constant-load levels and duration of the tests are set to be the same as what we have in the real data. The only difference from the subsequent real data analysis is that the data here are simulated with a prespecified θ. Throughout these two simulation scenarios, the procedure is as follows: we draw a sample with size N which is chosen to be close to the real data sample size. The proposal density

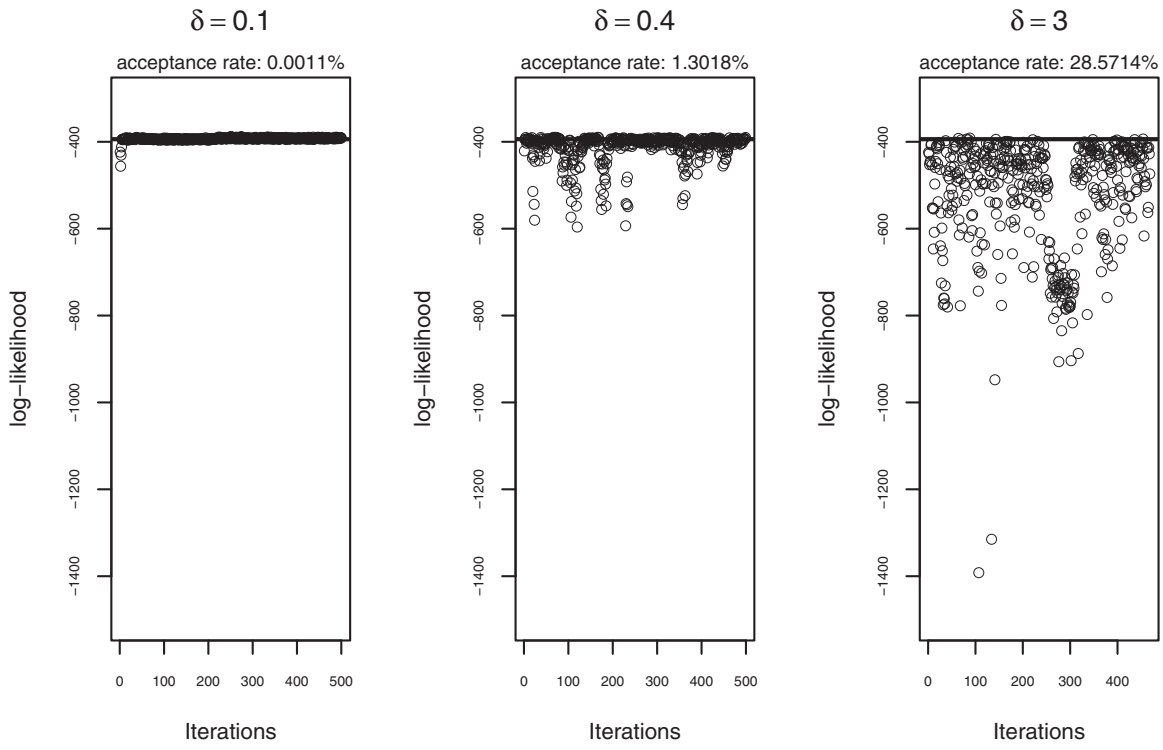

Figure 1. Log-likelihoods of t_{obs} for 500 ABC-MCMC samples of θ under different δ; the solid line is the log-likelihood of t_{obs} given the true θ. δ is the bandwidth of the kernel.

$g(\theta'|\theta_k)$ for the random-walk Metropolis–Hastings is $N(\theta_k, \Sigma)$, where $\Sigma = \text{diag}\{0.01, 0.01, 0.01, 0.01, 0.2, 0.01, 0.01, 0.01, 0.1, 0.01\}$ ($\text{diag}\{c_1, \ldots, c_n\}$ denotes the diagonal matrix with diagonal entries $c_1, \ldots, c_n$). We generate N observations with $\theta = (-7.50, 0.50, 3.20, 0.20, -22.00, 0.30, -1.00, 0.20, 0.15, 0.05)$. These parameter values are chosen from preliminary data analysis such that they produce data that are somewhat similar to the real data. We then run Algorithm 2 to obtain 500 posterior draws of θ with 100,000 burn-in iterations and thinning interval 10,000. The large thinning interval was used to eliminate autocorrelation in the MCMC samples. To explore the effect of δ, we run simulations for 30 different values of δ equally spaced between 0.1 and 3 and choose the one with the acceptance rate closest to 1% as our choice of δ.

To evaluate the quality of the sampled θ's, we can perform an approximate log-likelihood calculation on a small subset of the samples from the MCMC run, such as our thinned list of 500 posterior draws. To do so, we generate 100,000 failure times for each given θ and use kernel density estimation to calculate the log-likelihood for $\boldsymbol{t}_{obs}$. Recall that it is not practical to calculate the log-likelihood in this way during the MCMC for computing the M-H ratio, as to obtain an accurate estimate of the density we need to generate a large number of observations (e.g., 100,000), which is time-consuming. In contrast, for our algorithm we only need to generate the same number of observations as in the data at each MCMC iteration and hence runs very efficiently for exploring the parameter space.

Scenario 1: 4500/1Y In this scenario, we generate $N = 300$ observations with $\tau_c = 4500$ and the duration of the test being one year and fit this dataset with Algorithm 2.

In Figure 1, we have plotted these log-likelihoods for θ from three different δ values. It is clear that the choice of δ affects the quality of the simulation and goodness of the likelihood approximation. While small values of δ theoretically provide the best approximation, the extremely low acceptance rate renders $\delta = 0.1$ to be useless in practice. For large values of δ, the approximation is too crude which makes the accepted draws of θ unreliable from the likelihood perspective. The results show that $\delta = 0.4$ indeed works well, with both a reasonable acceptance rate and good approximation to the likelihood.

Table 1 shows five sampled parameter vectors that produce the highest log-likelihood values and Table 2 shows the posterior means, the posterior standard deviations, and the 95% posterior intervals for the parameters. From Table 1, it is clear that these parameter vectors are quite different yet their log-likelihoods (and log-posteriors, since the priors are mostly diffuse) are very similar. This indicates some of the model parameters are quite uncertain and the likelihood is flat over a wide range of values. Indeed, this shows that our ABC-MCMC algorithm is able to traverse the parameter space to find parameter vectors that can fit the observed data well, and so the high level of uncertainty is not a difficulty in practice for the algorithm. Figure 2 shows that the estimated densities $f_T(t)$ based on kernel smoothing for these parameter vectors are almost indistinguishable.

Scenario 2: 4500/1Y and 3000/4Y In practice, multiple test samples with different constant-load levels are used to help calibrate the parameters. So we simulate such a scenario as well to see how the estimation can improve. For this purpose, we generate a second independent dataset with $N = 200$ observations, $\tau_c = 3000$, and a test duration of 4 years. We then fit this

Table 1. Five sampled parameter vectors, log-likelihoods, and log-posteriors for the simulated data in Scenario 1. The true value of θ is shown in the top row. These five parameter vectors produce the highest log-likelihood values among the 500 posterior draws and *ll* are the log-likelihood values

	μ_a	σ_a	μ_b	σ_b	μ_c	σ_c	μ_n	σ_n	μ_{σ_0}	σ_{σ_0}	*ll*	log-*post*
θ	−7.50	0.50	3.20	0.20	−22.00	0.30	−1.00	0.20	0.15	0.05	−393.96	−418.27
$\hat{\theta}_1$	−8.22	0.45	3.99	0.10	−42.88	0.12	−1.57	0.34	−1.54	0.71	−389.71	−417.46
$\hat{\theta}_2$	−7.44	0.43	3.39	0.62	−30.22	0.55	−1.40	0.32	0.17	0.20	−389.78	−416.29
$\hat{\theta}_3$	−7.85	0.44	3.64	0.38	−38.24	0.18	−1.52	0.50	−0.48	0.11	−389.84	−415.97
$\hat{\theta}_4$	−8.02	0.43	3.91	0.58	−13.92	0.15	0.13	0.42	−0.79	0.24	−390.02	−415.26
$\hat{\theta}_5$	−7.44	0.44	3.26	0.40	−30.67	0.62	−1.37	0.27	0.23	0.28	−390.14	−416.51

Table 2. Statistics for the 500 ABC-MCMC samples in Scenario 1: posterior means, posterior standard deviations, and posterior 95% credible intervals based on the 0.025 and 0.975 quantiles

	Mean	SD	95% interval
μ_a	−7.69	0.31	(−8.26, −7.10)
σ_a	0.37	0.15	(0.09, 0.67)
μ_b	3.53	0.34	(2.90, 4.07)
σ_b	0.30	0.25	(0.06, 0.92)
μ_c	−24.67	8.76	(−41.89, −11.50)
σ_c	0.32	0.29	(0.06, 1.10)
μ_n	−0.83	0.65	(−1.77, 0.66)
σ_n	0.26	0.14	(0.07, 0.58)
μ_{σ_0}	−0.21	0.60	(−1.52, 0.76)
σ_{σ_0}	0.29	0.23	(0.07, 0.96)

dataset together with the dataset in Scenario 1 to obtain parameter estimates based on the combined data. To fit $D > 1$ datasets at the same time (in this scenario, $D = 2$), we apply the ABC approximation to Equation (7) for each dataset separately. So a corresponding minor change in the M-H acceptance ratio is needed. Using the proposal θ', we generate the multiple datasets with the different settings (i.e., N, τ_c, and the test duration) and calculate the summary statistics and the censored proportions. To calculate the M-H acceptance ratio, we multiply together the parts involving the summary statistics and the censored proportions, that is,

$$\alpha(\theta', \theta_k) = \min\left(1, \frac{\pi(\theta')g(\theta'|\theta_k)}{\pi(\theta_k)g(\theta_k|\theta')} \prod_{d=1}^{D} \frac{K_\delta\left(\boldsymbol{s}^{(d)} - \boldsymbol{s}_{obs}^{(d)}\right)}{K_\delta\left(\boldsymbol{s}_k^{(d)} - \boldsymbol{s}_{obs}^{(d)}\right)} \times \left(\frac{1 - \hat{p}_{t_c}^{(d)}}{1 - \hat{p}_{t_c,k}^{(d)}}\right)^{n^{(d)} - n_c^{(d)}} \left(\frac{\hat{p}_{t_c}^{(d)}}{\hat{p}_{t_c,k}^{(d)}}\right)^{n_c^{(d)}}\right),$$

where the superscript $(\cdot)^{(d)}$ denotes the values for the dth simulated dataset, $d = 1, \ldots, D$.

For this simulation, we chose $\delta = 1.1$ which gave an acceptance rate of 1.18%. The results are shown in Tables 3, 4, and Figure 3. In Figure 3, we show histograms for the two simulated datasets separately, and overlay the estimated densities computed from the parameter vectors in Table 3. As the figure shows, these parameters vectors each provide very good fits to both datasets simultaneously. To see how the estimation improves, we examined the standard deviations of the posterior draws of $\hat{\theta}$ in Tables 2 and 4 and the range of their log-likelihoods. Indeed, the posterior standard deviations in Scenario 2 are generally smaller than those in Scenario 1; as well, 95% of the log-likelihoods in Scenario 1 lie in the range (−494.77, −389.71) while 95% of the log-likelihoods in Scenario 2 lie in the tighter range (−1072.76, −1035.25), indicating that incorporating the additional dataset makes the estimation and our ABC algorithm more stable.

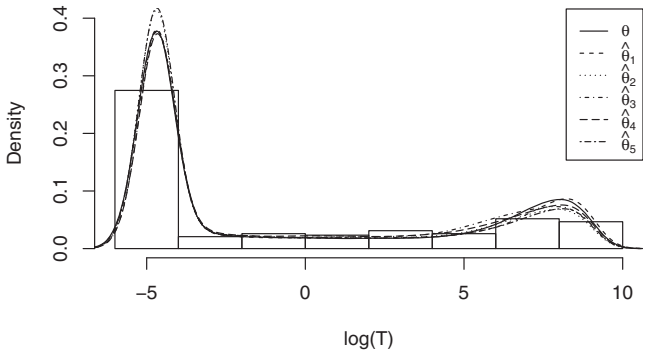

Figure 2. Histogram of simulated data (excluding censored observations) and estimated densities for the parameter vectors in Table 1.

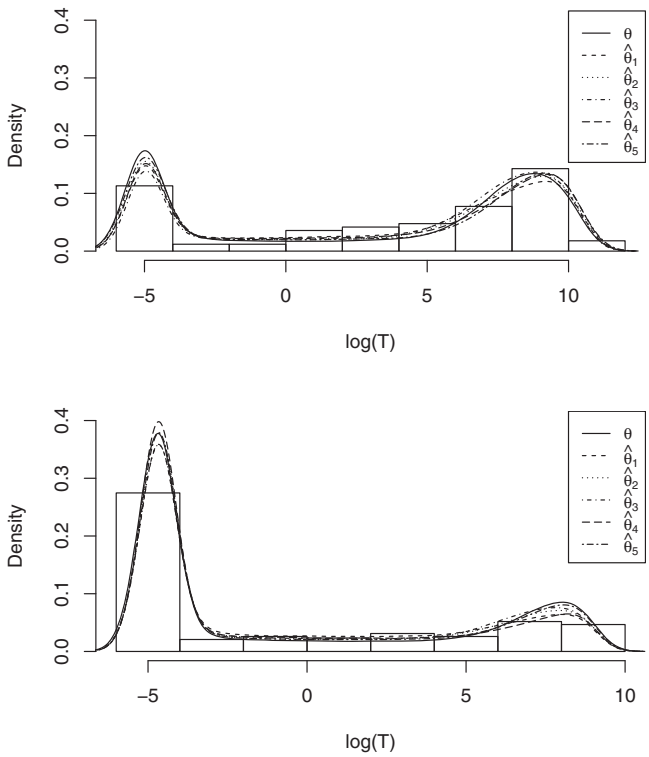

Figure 3. Histograms of simulated data (excluding censored observations) and estimated densities for the parameter vectors in Table 3. The top panel is the simulated 3000/4Y dataset and the bottom panel is the simulated 4500/1Y dataset.

Table 3. Five sampled parameter vectors, log-likelihoods, and log-posteriors from combining the two simulated datasets in Scenario 2. The true value of θ is shown in the top row. These five parameter vectors produce the highest log-likelihood values among the 500 posterior draws and *ll* are the log-likelihood values

	μ_a	σ_a	μ_b	σ_b	μ_c	σ_c	μ_n	σ_n	μ_{σ_0}	σ_{σ_0}	*ll*	log-*post*
θ	−7.50	0.50	3.20	0.20	−22.00	0.30	−1.00	0.20	0.15	0.05	−1040.83	−1065.14
$\hat{\theta}_1$	−8.09	0.52	3.48	0.41	−38.56	0.70	−1.21	0.53	−0.98	0.21	−1035.25	−1063.41
$\hat{\theta}_2$	−7.88	0.48	3.48	0.25	−17.33	0.24	−0.29	0.46	−0.39	0.20	−1035.31	−1060.06
$\hat{\theta}_3$	−7.88	0.41	3.47	0.48	−11.08	0.11	0.42	0.21	−0.43	0.79	−1035.52	−1060.64
$\hat{\theta}_4$	−8.04	0.45	3.58	0.26	−24.59	0.27	−0.73	0.41	−0.87	0.65	−1035.94	−1062.29
$\hat{\theta}_5$	−7.57	0.45	3.28	0.44	−11.55	0.07	0.26	0.19	0.08	0.11	−1036.02	−1059.60

4. Data Analysis

The illustrative real data example comes from a duration-of-load experiment performed on visually graded 2x6 Western Hemlock, which was first analyzed in Foschi and Barrett (1982). The experimental data consist of three groups, and the standard ramp-loading rate $k_s = 388, 440$psi/hour was used throughout:

(1) A set of 300 pieces was subject to a constant-load test with $\tau_c = 4500$psi for a duration of 1 year. In total, 56 pieces failed during the initial portion of the test, 98 failed during the 1-year constant-load period, and 146 survived to the end of the 1-year at which point the test was truncated.

(2) A set of 198 pieces was subject to a constant-load test with $\tau_c = 3000$psi for a duration of 4 years. In total, 4 pieces failed during the initial portion of the test, 42 failed during the 4-year constant-load period, and 152 survived to the end of the 4-years at which point the test was truncated.

(3) A set of 139 pieces was subject to the ramp-load test, that is, $\tau_c = +\infty$ in Equation (2). The sample mean of short-term strength τ_s in this set was 6936psi, and sample SD 2833psi.

To analyze the data, we followed the same procedure as described in Section 3 for multiple datasets and chose $\delta = 1.3$, which gave an overall ABC-MCMC acceptance rate of 0.88%. To set starting values for the algorithm, we used the NLS estimates from Foschi and Yao (1986) as guidance, modified according to our parameterization. Table 5 shows the five parameter vectors with the highest log-likelihood values and Table 6 shows the posterior means, the posterior standard deviations, and the 95% posterior intervals for the parameter vectors. The histogram and the empirical cumulative distribution function (ecdf) of the data, along with the corresponding smoothed densities and cumulative distribution functions (CDFs) for the parameter vectors from Table 5 are shown in Figures 4 and 5. The results show that these parameter vectors indeed provide a very good fit to the data, and capture the variability in the individual parameters.

As noted by a reviewer, not all five random effects may be necessary for fitting the model to a particular dataset. Indeed, the variabilities in the piece-specific random effects b, c, n, σ_0

Table 4. Statistics for the 500 ABC-MCMC samples in Scenario 2: posterior means, posterior standard deviations, and posterior 95% credible intervals based on the 0.025 and 0.975 quantiles

	Mean	SD	95% interval
μ_a	−7.72	0.23	(−8.16, −7.25)
σ_a	0.44	0.11	(0.22, 0.66)
μ_b	3.22	0.33	(2.62, 3.81)
σ_b	0.26	0.19	(0.06, 0.74)
μ_c	−16.84	5.49	(−30.86, −10.49)
σ_c	0.28	0.19	(0.07, 0.81)
μ_n	−0.27	0.45	(−1.21, 0.65)
σ_n	0.26	0.16	(0.06, 0.61)
μ_{σ_0}	−0.21	0.39	(−1.08, 0.44)
σ_{σ_0}	0.33	0.27	(0.07, 1.09)

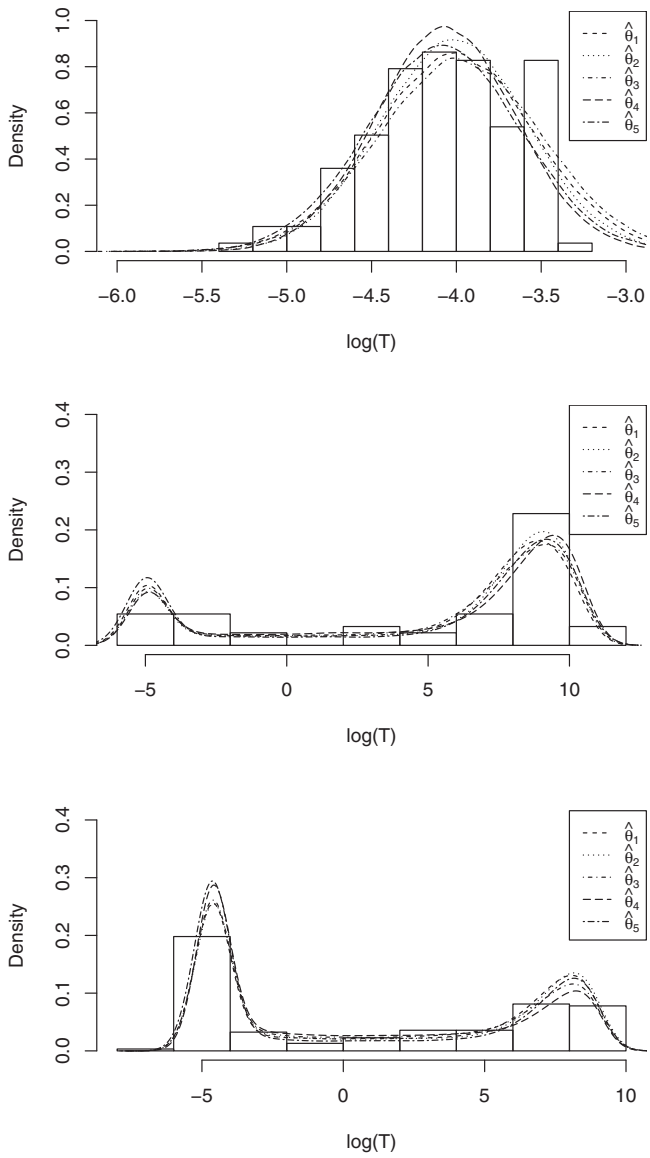

Figure 4. Histograms of the real datasets (excluding censored observations) and estimated densities for the parameter vectors in Table 5. The top panel is the ramp-load dataset, the middle panel is the real 3000/4Y dataset, and the bottom panel is the real 4500/1Y dataset.

Table 5. Five sampled parameter vectors, log-likelihoods, and log-posteriors for the real data. These five parameter vectors produce the highest log-likelihood values among the 500 posterior draws and *ll* are the log-likelihood values

	μ_a	σ_a	μ_b	σ_b	μ_c	σ_c	μ_n	σ_n	μ_{σ_0}	σ_{σ_0}	*ll*	log-*post*
$\hat{\theta}_1$	−7.48	0.40	3.27	0.16	−17.42	1.27	−0.70	0.09	0.52	0.27	−632.72	−666.22
$\hat{\theta}_2$	−7.76	0.48	3.21	0.18	−21.96	0.29	−1.00	0.20	0.15	0.07	−632.89	−664.71
$\hat{\theta}_3$	−7.74	0.41	3.45	0.28	−17.06	0.40	−0.48	0.23	0.13	0.10	−633.20	−665.98
$\hat{\theta}_4$	−7.88	0.42	3.33	0.11	−17.72	0.19	−0.39	0.26	−0.13	0.19	−633.37	−665.28
$\hat{\theta}_5$	−7.68	0.44	3.23	0.10	−22.12	0.10	−0.99	0.15	0.29	0.16	−633.75	−664.54

appear to be low here, as indicated by the small magnitudes of the corresponding parameters $\sigma_b, \sigma_c, \sigma_n, \sigma_{\sigma_0}$ in Table 6. Appendix C uses our ABC-MCMC procedure to investigate whether a simplified model, with fewer random effects, can reasonably fit this specific dataset.

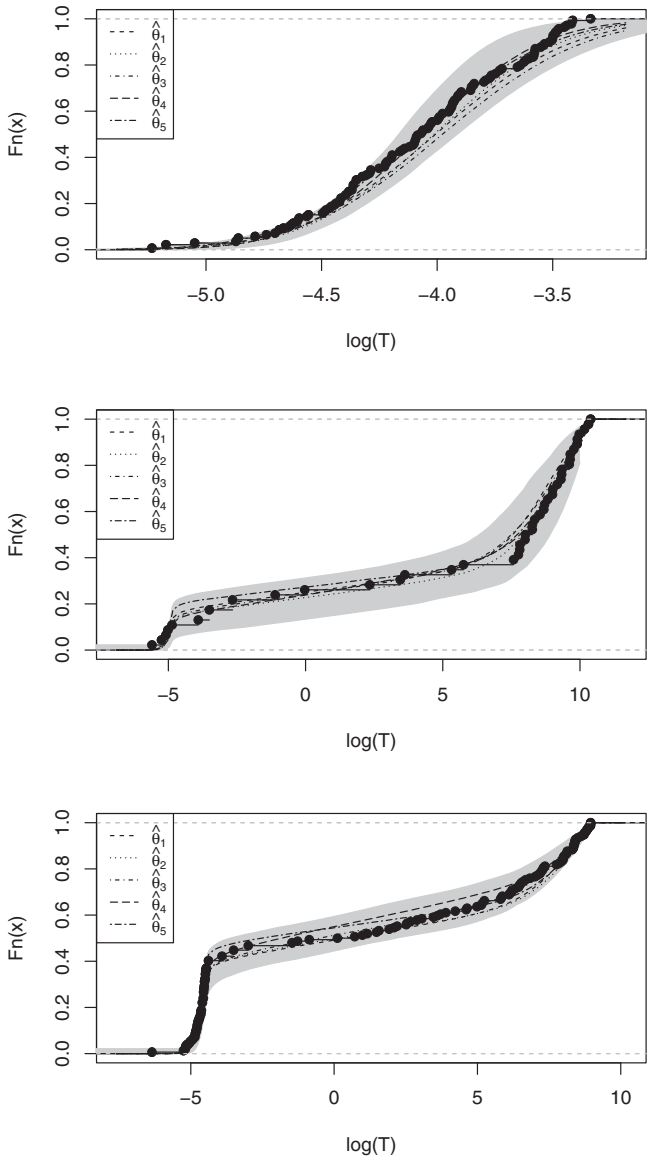

Figure 5. Empirical CDF of the real data (excluding censored observations), and CDFs computed from the parameter vectors in Table 5. The top panel is the ramp-load dataset, the middle panel is the 3000/4Y dataset, and the bottom panel is the 4500/1Y dataset. The gray area is the 95% posterior interval of the estimated empirical CDFs.

5. Assessing Long-Term Lumber Reliability

5.1 Reliability Analysis for Live Loads

The key application of the fitted ADM is to assess the long-term reliability of lumber, given a characterization of the load profile $\tau(t)$ that will be encountered in service. To present this assessment, we first overview the construction of an example live load profile and the key elements of a reliability analysis. The reader may refer to the Appendices for additional background and details of the results used.

Structures encounter different live load patterns, such as owner occupancy in residential units, office occupancy in commercial buildings, and snow loads on roofs that vary by region. A more comprehensive discussion and comparison of these live loads can be found in Foschi, Folz, and Yao (1989). For the following demonstration, we adopt the residential loads model for $\tau(t)$, $t \geq 0$ presented therein. The load is stochastic and defined as follows,

$$\tau(t) = \phi R_o \frac{\gamma \tilde{D}_d + \tilde{D}_s(t) + \tilde{D}_e(t)}{\gamma \alpha_d + \alpha_l}. \tag{8}$$

Following the National Building Code of Canada (NBCC) standards document CAN/CSA-O86, we assume that $\gamma = 0.25$, $\alpha_d = 1.25$, $\alpha_l = 1.5$. The value R_o is the characteristic value depending on the lumber population, which in our example will be the fifth percentile of the strength distribution of a hemlock species $R_o = 2722$ psi. The parameter ϕ is called the *performance factor* and plays a fundamental role in reliability modeling, as a multiplicative factor applied to the load level.

The specifications for the load components in Equation (8) from Foschi, Folz, and Yao (1989) are as follows. The normalized dead load for the weight of the structure $\tilde{D}_d$ is assumed to be a random variable $\tilde{D}_d \sim N(1, 0.01)$. The sustained load $\tilde{D}_s(t)$ and the extraordinary load $\tilde{D}_e(t)$ are two independent

Table 6. Statistics for the 500 ABC-MCMC samples in real data analysis: posterior means, posterior standard deviations, and posterior 95% credible intervals based on the 0.025 and 0.975 quantiles

	Mean	SD	95% interval
μ_a	−7.76	0.23	(−8.23, −7.35)
σ_a	0.40	0.07	(0.25, 0.55)
μ_b	3.26	0.25	(2.75, 3.73)
σ_b	0.20	0.14	(0.06, 0.62)
μ_c	−20.94	6.15	(−34.79, −12.07)
σ_c	0.28	0.28	(0.06, 1.17)
μ_n	−0.68	0.43	(−1.40, 0.20)
σ_n	0.25	0.19	(0.06, 0.75)
μ_{σ_0}	0.06	0.32	(−0.67, 0.61)
σ_{σ_0}	0.21	0.11	(0.06, 0.47)

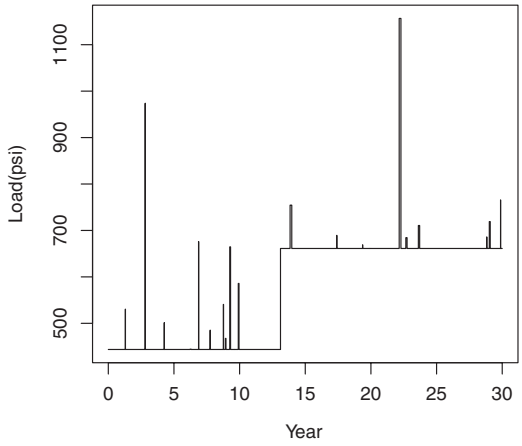

Figure 6. An example residential load profile with $\phi = 1$.

processes. The sizes of the loads are modeled using gamma distributions $G(k, \theta)$ where k and θ represent the shape and scale parameters. The random times between and during live load events are modeled using exponential distributions $\text{Exp}(\lambda)$ with mean λ^{-1}. Parameters for these models were previously fitted using survey data (Corotis and Doshi 1977; Chalk and Corotis 1980; Harris, Bova, and Corotis 1981).

The process $\tilde{D}_s(t)$ consists of a sequence of successive periods of sustained occupancy each with iid duration $T_s \sim \text{Exp}(1/0.1)$. During these periods of occupancy $\tilde{D}_{ls} \sim G(3.122, 0.0481)$ iid. The process $\tilde{D}_e(t)$ consists of brief periods of extraordinary loads, separated by longer periods with no load $T_e \sim \text{Exp}(1.0)$ of expected duration 1 year. When extraordinary loads occur, they last for iid periods of random duration $T_p \sim \text{Exp}(1/0.03835)$. The normalized loads $\tilde{D}_{le}$ during these brief periods are iid with gamma distribution $\tilde{D}_{le} \sim G(0.826, 0.1023)$.

An example of a simulated 30-year load profile according to these settings is shown in Figure 6.

For a reliability analysis, the required service time for a piece of lumber is assumed to be 30 years. Reliability is reported in terms of the *reliability index*, defined as

$$\beta = -\Phi^{-1}(p_f),$$

where p_f is the probability of failure during the service time and Φ is the standard Normal CDF. See Madsen, Krenk, and Lind (2006) for more details. Clearly β and ϕ must be related, since larger loads (higher ϕ) are associated with more failures (lower β).

To simulate the damage accumulation process for a single random specimen, its random effects are sampled along with a realization of $\tau(t)$. Then according to the ADM, the specimen is deemed to have failed if for some $t \leq 30$, $1 \leq \alpha(t)$ and the associated survival time would be the smallest t for which that is true. Based on a large number of replications, the estimated probability of failure after 30 years, $\hat{p}_f$, is obtained. From that estimate we compute

$$\hat{\beta} = -\Phi^{-1}(\hat{p}_f).$$

By repeating this procedure for successive values of ϕ, the functional relationship between β and ϕ can be estimated.

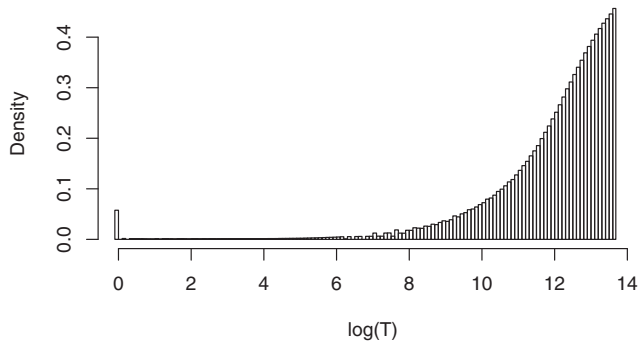

Figure 7. Histogram of the posterior distribution of time-to-failure with a $\phi = 3$ load profile, for failures that occur within the first 100 years.

5.2 Analysis Results

The failure time from the Canadian model cannot be solved analytically for an arbitrary loading profile $\tau(t)$, so we obtain its numerical solution using `odeint` in the C++ Boost library. This library provides a wide range of ordinary differential equation (ODE) solvers and we use the five-step Adams–Bashforth method for the sake of efficiency.

Based on our Bayesian framework, the posterior cumulative probability for the future time-to-failure T_f can be estimated using the MCMC samples θ_i of θ,

$$\begin{aligned} P(T_f < t|\boldsymbol{t}_{\text{obs}}) &\approx \frac{1}{n_i n_j} \sum_{i=1}^{n_i} \sum_{j=1}^{n_j} P(T_f < t|\theta_i, \tau_{ij}) \\ &\approx \frac{1}{n_i n_j} \sum_{i=1}^{n_i} \sum_{j=1}^{n_j} P(T_f < t|a_{ij}, b_{ij}, c_{ij}, n_{ij}, \sigma_{0,ij}, \tau_{ij}) \\ &\approx \frac{1}{n_i n_j} \sum_{i=1}^{n_i} \sum_{j=1}^{n_j} I_{\{t:t_{f,ij}<t\}}(t), \end{aligned}$$

where each $\tau_{ij} = \tau_{ij}(t)$ is an independent realization of the stochastic load profile, $a_{ij}, b_{ij}, c_{ij}, n_{ij}, \sigma_{0,ij}$ are independent draws of the piece-specific random effects from Equation (5) conditioning on θ_i, and $t_{f,ij}$ is the solution to the ADM given $a_{ij}, b_{ij}, c_{ij}, n_{ij}, \sigma_{0,ij}, \tau_{ij}$.

Hence our simulation procedure is as follows: for each of the $n_i = 500$ draws of θ in Section 4, we generate a, b, c, n, σ_0 using Equation (5). Then we solve the Canadian ADM for the time-to-failure T_f with this a, b, c, n, σ_0 and a randomly generated load profile from Equation (8) with the given ϕ. We replicate this $n_j = 100,000$ times for each draw of θ. For example, the posterior distribution of the time-to-failure T_f given the data $\boldsymbol{t}_{\text{obs}}$ with a $\phi = 3$ load profile is shown in Figure 7. Note that there is a small peak at the bottom of the histogram; these correspond to the weakest pieces of lumber that do not survive the initial loads under this scenario.

This procedure provides the estimated probability of failure $\hat{p}_f$ by the end of 30 years and the associated reliability index $\hat{\beta}$. To quantify the DOL effect, we also calculate the reliability index assuming there is no DOL effect. When there is no DOL effect, a piece of lumber breaks if the maximum load exceeds its short-term strength τ_s during the 30-year period. The result is shown in Figure 8. We also replicate the result in Foschi, Folz, and Yao (1989) by generating a, b, c, n, σ_0 using their estimates

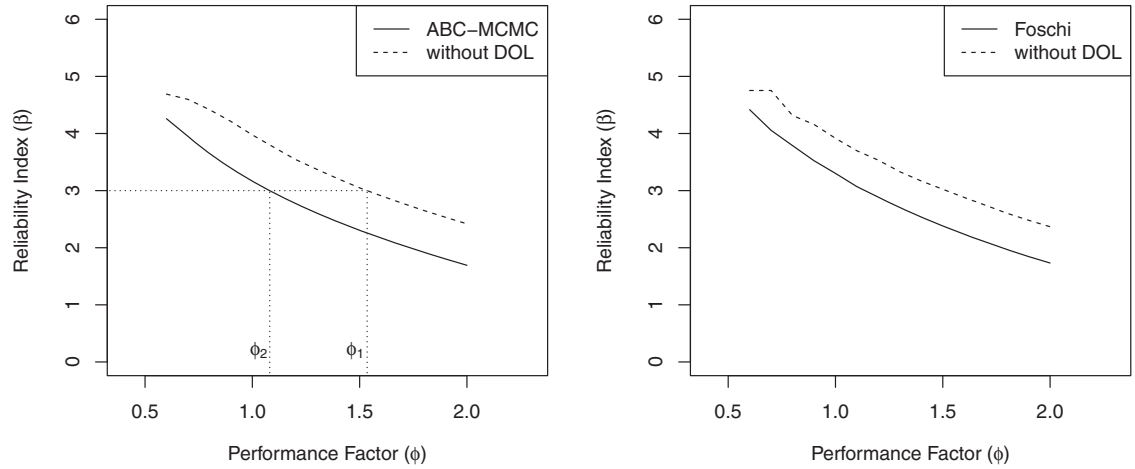

Figure 8. $\phi - \beta$ relationship for ABC-MCMC and Foschi's estimates. When the DOL effect is considered, it can be seen that more failures are expected (and thus a lower reliability index) across all values of ϕ due to damage accumulated from sustained loads. The ABC-MCMC approach provides slightly lower estimates of β overall compared to Foschi's original estimates.

Table 7. The adjustment factors K_D for ABC-MCMC and Foschi's estimates

	ABC-MCMC				Foschi		
	ϕ_2	ϕ_1	K_D	95% Interval	ϕ_2	ϕ_1	K_D
$\beta = 2.5$	1.37	1.93	0.71	(0.56, 0.81)	1.42	1.88	0.76
$\beta = 3.0$	1.08	1.53	0.71	(0.53, 0.81)	1.14	1.52	0.75
$\beta = 3.5$	0.86	1.23	0.70	(0.49, 0.82)	0.91	1.22	0.75

and parameterization. Then for a fixed β, we can measure the DOL effect by taking the ratio of the two corresponding performance factors ϕ_1 and ϕ_2 as indicated for $\beta = 3$ in Figure 8. Foschi, Folz, and Yao (1989) defined this ratio as the adjustment factor K_D, that is,

$$K_D = \frac{\phi_2}{\phi_1},$$

where ϕ_1 and ϕ_2 are the performance factors corresponding to the specified value of β when DOL effect is absent and present, respectively. The result is shown in Table 7. For our method, we are also able to calculate the 95% posterior interval for K_D using the MCMC samples. The point estimates shown for our approach are the posterior means.

We find that our approach provides a more conservative estimate of reliability, while the result of Foschi, Folz, and Yao (1989) is well within the range that would be expected due to uncertainty from parameter estimation. The ability to produce interval estimates is an important feature of our method, as such intervals were not previously available using the Foschi approach.

6. Discussion and Conclusions

In this article, we presented a Bayesian framework for estimating the parameters and quantifying the uncertainty in the parameters for the Canadian ADM. We adapted an ABC algorithm to handle the computational challenges. Using the fitted model, we presented an application to reliability analysis using the posterior distributions of the parameters.

Our approach provides posterior probability intervals that quantify the DOL effect, in particular the important adjustment factor K_D; such interval estimates could not be obtained by the approach in Foschi, Folz, and Yao (1989). We note that both the number (five) and structure of the random effects (independent log-normals) adopted here were inherited from how the Canadian ADM was previously used. Future work can apply this Bayesian framework to other forms of ADMs and explore alternative or reduced parameterizations. As indicated by Appendix C, the specific dataset considered in this article can be fit reasonably well with fewer random effects; in this case the posterior interval widths of the associated reliability estimates remained similar. More generally, if a well-informed dependence structure or constraints could be placed on the parameters, the posterior intervals of the estimates may become more precise, along with those of the resulting reliability predictions. The computational approach we presented can easily handle such refinements to the model, as long as one can simulate draws from the random effects distributions. These aspects warrant further study with data from additional duration-of-load experiments. Other forms of future live loads can also be added to the analysis—such as snow, wind, and earthquakes—so as to obtain more realistic different stochastic load patterns for $\tau(t)$.

Our work also shows that ABC-MCMC indeed is a promising approach for complicated models, in particular, models involving differential equations that are widely used in engineering applications. The absence of an analytic solution and intractability of the likelihood can pose difficulties for applying traditional statistical methods in such models, especially when the equations involve latent random effects. With this approach, the only requirement to perform statistical analysis and quantify estimation uncertainty is the ability to solve the differential equations numerically given the parameters. The general ABC-MCMC methodology is also extensible. Here, we introduced an adapted version suitable for handling the censoring seen in our failure time data.

The results presented also indicate that ABC-MCMC can be especially powerful when the likelihood computation is very costly, but not impossible. In that case, an ABC-MCMC sampler that bypasses the likelihood can quickly explore the parameter space to find good candidates of the parameter vector that fit the data well, as our examples show. The costly likelihood

Table C.1. Five sampled parameter vectors, log-likelihoods, and log-posteriors for the real data using the reduced model. These five parameter vectors produce the highest log-likelihood values among the 500 posterior draws and *ll* are the log-likelihood values

	μ_a	σ_a	μ_b	μ_c	μ_n	μ_{σ_0}	*ll*	log-*post*
$\hat{\theta}_1$	−7.79	0.45	3.34	−12.79	0.05	0.06	−633.01	−656.75
$\hat{\theta}_1$	−7.72	0.43	3.11	−9.68	0.68	0.11	−634.07	−657.67
$\hat{\theta}_1$	−7.61	0.40	3.38	−11.26	0.21	0.32	−634.58	−658.14
$\hat{\theta}_1$	−7.57	0.45	3.27	−16.30	−0.52	0.38	−634.75	−658.61
$\hat{\theta}_1$	−7.82	0.48	3.31	−12.81	−0.03	0.07	−634.85	−658.64

computation can then be applied to a subset of the sampled parameter vectors to directly assess the goodness of the ABC approximation. For our ADM application, we verified that our parameter estimates are sensible by using a simple but computationally expensive brute-force simulation to evaluate the likelihood.

Appendix A: Canadian Model Derivation

These results are based on those derived in Wong and Zidek (2018). For a ramp-load test using the standard loading rate $k = k_s$, then we have $\tau(t) = k_s t$, $\tau_s = kT_s$, and

$$\frac{d}{dt}\alpha(t)\mu = [akT_s(t/T_s - \sigma_0)_+]^b + [ckT_s(t/T_s - \sigma_0)_+]^n \alpha(t).$$

Define the integrating factor

$$H(t) = \exp\left\{\int -\frac{1}{\mu}\left[ckT_s\left(\frac{t}{T_s} - \sigma_0\right)\right]^n dt\right\}$$
$$= \exp\left\{-\frac{1}{\mu}(ckT_s)^n \frac{T_s}{n+1}\left(\frac{t}{T_s} - \sigma_0\right)^{n+1}\right\}.$$

Then

$$\frac{d}{dt}[\alpha(t)H(t)] = \frac{1}{\mu}\cdot H(t)\left[akT_s\left(\frac{t}{T_s} - \sigma_0\right)\right]^b.$$

No damage is accumulated until $t = \sigma_0 T_s$, so integrating we obtain

$$\alpha(T_s)H(T_s) - \alpha(\sigma_0 T_s)H(\sigma_0 T_s) = \int_{\sigma_0 T_s}^{T_s} \frac{1}{\mu}\cdot H(t)\left[akT_s\left(\frac{t}{T_s} - \sigma_0\right)\right]^b dt.$$

Finally, the change of variables $u = -\log H(t)$ yields Equation (3), where we then recognize the integral to be the lower incomplete Gamma function, which can be evaluated numerically using standard mathematical libraries.

Appendix B: Reliability Analysis for Live Loads

Reliability assessment is based on the performance equation

$$G = C - D, \tag{B.1}$$

where both the future demand to be made on a random piece of lumber D and its capacity to meet that demand C depend on a random vector of random design variables that after a suitable transformation have a standard multivariate normal distribution. A Laplace approximation yields the probability of failure

$$p_f = P(G \le 0) \approx 1 - \Phi(\beta),$$

where β is called the *reliability index*. See Madsen, Krenk, and Lind (2006) for more details.

The random future load to which that piece will be exposed is the sum of two random components, the dead load D_d and the live load D_l. For illustrative purposes, we adopt the generative model of future loads for $\tau(t)$, $\tilde{}t \ge 0$ presented in Foschi, Folz, and Yao (1989). We briefly review the stochastic models with which the future loads are simulated and how those load levels are used to construct plots for reliability assessment.

At the basis of the model are certain specified constants called design values, which are in the National Building Code of Canada (NBCC) standards document CAN/CSA-O86: d_{nd} and d_{nl}. The design values for the dead and live loads are then modeled as the constants $d_d = \alpha_d d_{nd}$ and $d_l = \alpha_l d_{nl}$, respectively, for specified parameters $\alpha_d = 1.25$ and $\alpha_l = 1.5$. The design load is the constant $d_d + d_l$.

The corresponding constant for capacity C is based on the characteristic value R_o for a given lumber population. Typically it is set to be a lower percentile of the strength distribution, for example, the fifth percentile. The design capacity is then $\phi' R_o$ for some constant ϕ', with corresponding design performance $\phi' R_o - (d_d + d_l)$. The design capacity will equal or exceed the design demand if ϕ' is set at the ϕ for which

$$\phi R_o - (d_d + d_l) = 0. \tag{B.2}$$

Another design value of importance is the dead to live load ratio $\gamma = d_{nd}/d_{nl}$, which is typically 0.25. A little algebra then shows

$$d_{nl} = \frac{\phi R_o}{\gamma\alpha_d + \alpha_l}. \tag{B.3}$$

The parameter ϕ is called the *performance factor* and like β plays a fundamental role in reliability modeling.

However in reality the dead and live loads are random and their distributions must now be specified. This is done by using the design values as a baseline and normalizing the loads as $\tilde{D}_d = D_d/d_{nd}$ and $\tilde{D}_l = D_l/d_{nl}$. We will confine our analysis in this article to live residential loads, which is one of the many cases explored in Foschi, Folz, and Yao (1989). Hence we adopt their stochastic load specifications, by first assuming that $\tilde{D}_d \sim N(1, 0.01)$, which is constant for the life of the structure.

The live loads are modeled as a sum of loads from two independent processes: sustained and extraordinary. The sizes of the loads are modeled using gamma distributions $G(k, \theta)$ where k and θ represent the shape and scale parameters. The random times between and during live load events are modeled using exponential distributions $Exp(\lambda)$ with mean λ^{-1}. Hence, the normalized live load at time t is given by the stochastic process $\tilde{D}_l(t) = \tilde{D}_s(t) + \tilde{D}_e(t)$, where $\tilde{D}_s$ and $\tilde{D}_e$ are the normalized sustained and extraordinary loads, respectively.

The combined normalized dead and live loads are then converted to actual load levels $\tau(t)$. Applying Equation (B.3) it is easily shown that

$$\tau(t) = \phi R_o \frac{\gamma\tilde{D}_d + \tilde{D}_s(t) + \tilde{D}_e(t)}{\gamma\alpha_d + \alpha_l}.$$

Table C.2. Statistics for the 500 ABC-MCMC samples in real data analysis under the reduced model: posterior means, posterior standard deviations, and posterior 95% credible intervals based on the 0.025 and 0.975 quantiles

	Mean	SD	95% interval
μ_A	−7.95	0.28	(−8.45, −7.41)
σ_A	0.46	0.07	(0.34, 0.61)
μ_b	3.40	0.33	(2.82, 4.03)
μ_C	−14.17	5.06	(−24.78, −8.28)
μ_n	0.14	0.75	(−1.06, 1.42)
μ_{σ_0}	−0.25	0.55	(−1.63, 0.54)

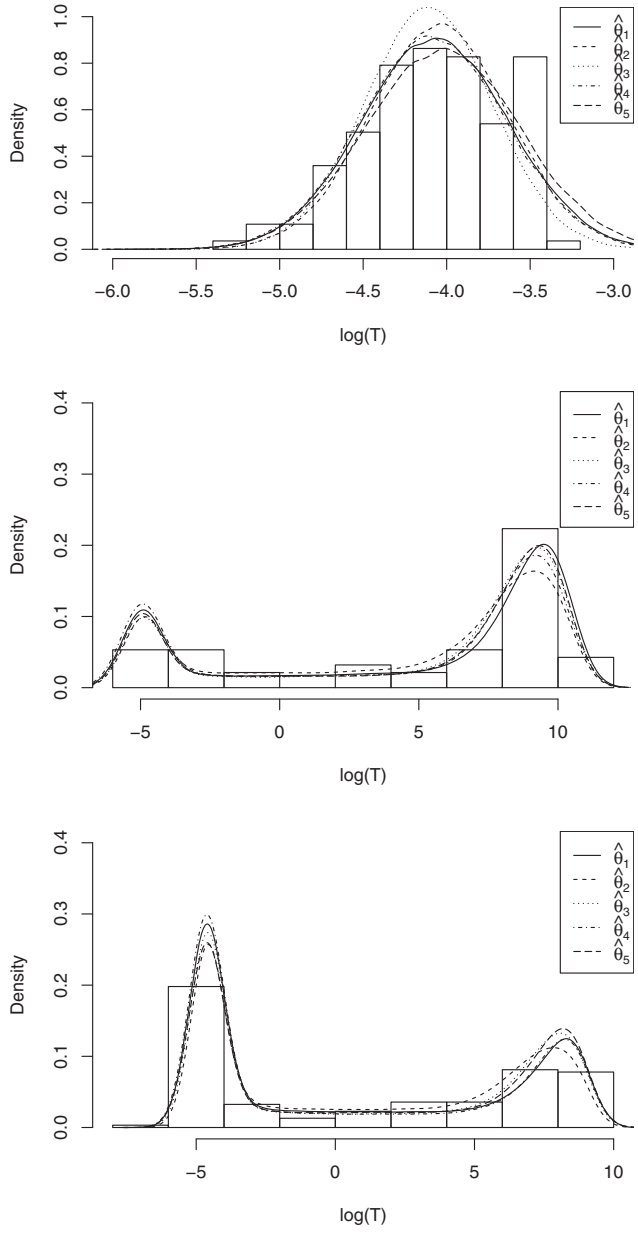

Figure C.1. Histograms of the real datasets (excluding censored observations) and estimated densities for the parameter vectors in Table C.1. The top panel is the ramp-load dataset, the middle panel is the real 3000/4Y dataset, and the bottom panel is the real 4500/1Y dataset.

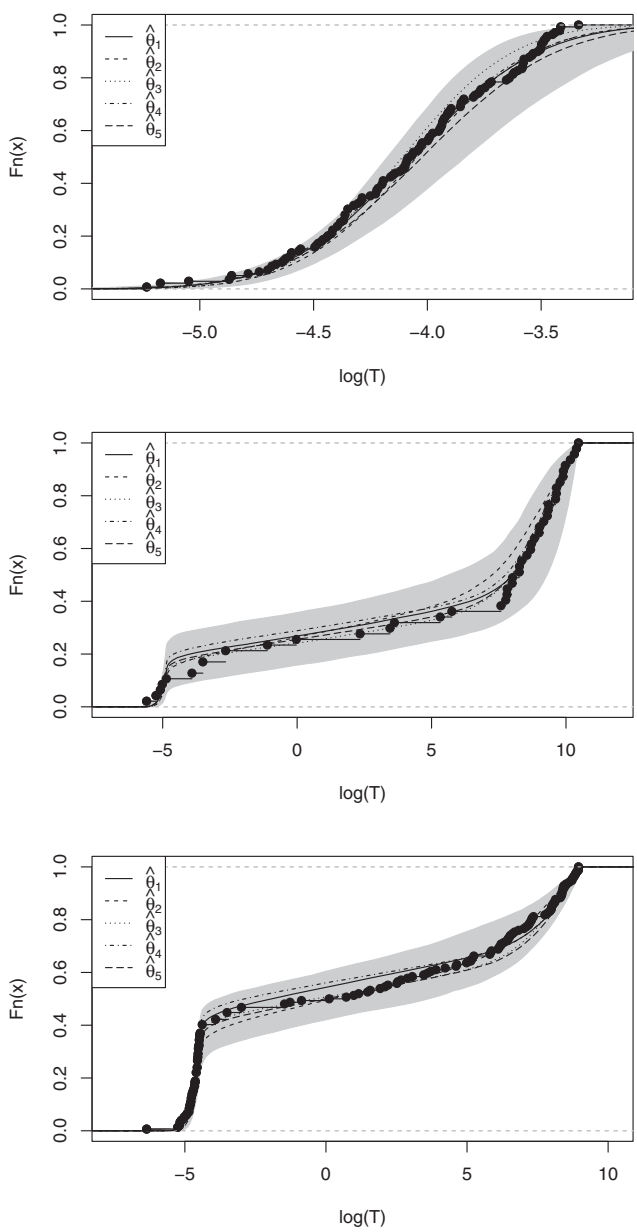

Figure C.2. Empirical CDF of the real data (excluding censored observations), and CDFs computed from the parameter vectors in Table C.1. The top panel is the ramp-load dataset, the middle panel is the 3000/4Y dataset, and the bottom panel is the 4500/1Y dataset. The gray area is the 95% posterior interval of the estimated empirical CDFs.

Appendix C: Assessing the Random Effects

It was noted by a reviewer that not all five random effects may be necessary for fitting the Canadian ADM to a particular dataset. To investigate this for the specific dataset considered in the article, we successively removed one random effect at a time (by setting the corresponding σ of its log-normal distribution to be zero) and refitted the model using our ABC-MCMC approach. We then examined the log-likelihood values (Table C.1) and ecdf plots (Figures C.1 and C.2) to assess the goodness of fit. For this

Table C.3. The adjustment factors K_D under the reduced model

	ABC-MCMC			
	ϕ_2	ϕ_1	K_D	95% Interval
$\beta = 2.5$	1.37	1.78	0.77	(0.61, 0.86)
$\beta = 3.0$	1.08	1.44	0.75	(0.55, 0.89)
$\beta = 3.5$	0.85	1.13	0.76	(0.58, 0.92)

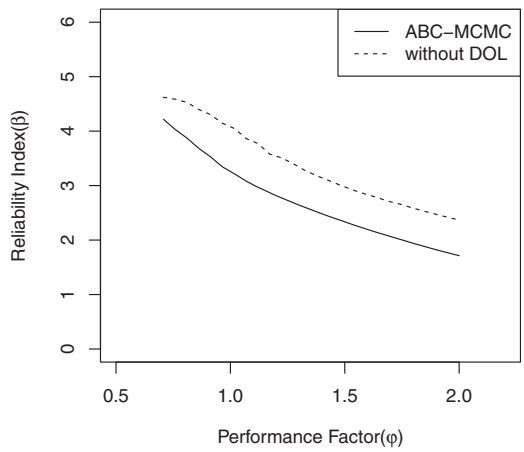

Figure C.3. $\phi - \beta$ relationship under the reduced model.

dataset, the random effects for b, c, n, σ_0 could all be removed without substantially worsening the fit. Parameter estimates are shown in Table C.2.

Following the procedure in Section 5, we also computed the reliability estimates corresponding to this fit, to assess whether the results are sensitive to this modification to the model. The results are shown in Table C.3 and Figure C.3. The point estimates for K_D are closer to Foschi's values, while the widths of the posterior interval are similar and have significant overlap with those in Table 7. Thus, we conclude that the final reliability assessments based on these data are robust to the model assumed.

Acknowledgments

The work reported in this manuscript was partially supported by FPInnovations and a CRD grant from the Natural Sciences and Engineering Research Council of Canada. The data analyzed in this article were provided by FPInnovations. The authors are greatly indebted to Conroy Lum and Erol Karacabeyli from FPInnovations for their extensive advice during the conduct of the research reported herein.

References

Allingham, D., King, R., and Mengersen, K. L. (2009), "Bayesian Estimation of Quantile Distributions," *Statistics and Computing*, 19, 189–201. [4]

Bae, S. J., and Kvam, P. H. (2004), "A Nonlinear Random-Coefficients Model for Degradation Testing," *Technometrics*, 46, 460–469. [3]

Barrett, J., and Foschi, R. (1978), "Duration of Load and Probability of Failure in Wood. Part II. Constant, Ramp, and Cyclic Loadings," *Canadian Journal of Civil Engineering*, 5, 515–532. [1]

Beaumont, M. A., Zhang, W., and Balding, D. J. (2002), "Approximate Bayesian Computation in Population Genetics," *Genetics*, 162, 2025–2035. [3]

Chalk, P. L., and Corotis, R. B. (1980), "Probability Model for Design Live Loads," *Journal of the Structural Division*, 106, 2017–2033. [9]

Corotis, R. B., and Doshi, V. A. (1977), "Probability Models for Live-Load Survey Results," *Journal of the Structural Division*, 103, 1257–1274. [9]

Fearnhead, P., and Prangle, D. (2012), "Constructing Summary Statistics for Approximate Bayesian Computation: Semi-Automatic Approximate Bayesian Computation," *Journal of the Royal Statistical Society*, Series B, 74, 419–474. [3,4]

Foschi, R. O. (1979), "A Discussion on the Application of the Safety Index Concept to Wood Structures," *Canadian Journal of Civil Engineering*, 6, 51–58. [1]

Foschi, R. O., and Barrett, J. D. (1982), "Load-Duration Effects in Western Hemlock Lumber," *Journal of the Structural Division*, 108, 1494–1510. [7]

Foschi, R. O., Folz, B., and Yao, F. (1989), *Reliability-Based Design of Wood Structures* (Vol. 34), Vancouver, BC: Department of Civil Engineering, University of British Columbia. [1,2,3,8,9,10,11]

Foschi, R. O., and Yao, F. Z. (1986), "Another Look at Three Duration of Load Models." in *IUFRO Wood Engineering Group Meeting*, Florence, Italy, International Council for Research and Innovation in Building and Construction, Paper no. 19-9-1. [1,2,7]

Fridley, K. J., Tang, R., and Soltis, L. A. (1992), "Load-Duration Effects in Structural Lumber: Strain Energy Approach," *Journal of Structural Engineering*, 118, 2351–2369. [2]

Gerhards, C. (1979), "Time-Related Effects of Loading on Wood Strength: A Linear Cumulative Damage Theory," *Wood Science*, 11, 139–144. [1]

Gerhards, C., and Link, C. (1987), "A Cumulative Damage Model to Predict Load Duration Characteristics of Lumber," *Wood and Fiber Science*, 19, 147–164. [1,2]

Harris, M. E., Bova, C. J., and Corotis, R. B. (1981), "Area-Dependent Processes for Structural Live Loads," *Journal of the Structural Division*, 107, 857–872. [9]

Hoffmeyer, P., and Sørensen, J. D. (2007), "Duration of Load Revisited," *Wood Science and Technology*, 41, 687–711. [1]

Joyce, P., and Marjoram, P. (2008), "Approximately Sufficient Statistics and Bayesian Computation," *Statistical Applications in Genetics and Molecular Biology*, 7, Article 26. [3]

Li, Y., and Lam, F. (2016), "Reliability Analysis and Duration-of-Load Strength Adjustment Factor of the Rolling Shear Strength of Cross Laminated Timber," *Journal of Wood Science*, 62, 492–502. [2]

Madsen, H. O., Krenk, S., and Lind, N. C. (2006), *Methods of Structural Safety*, Mineola, NY: Courier Corporation. [9,11]

Pinheiro, J. C., and Bates, D. M. (1995), "Approximations to the Log-Likelihood Function in the Nonlinear Mixed-Effects Model," *Journal of Computational and Graphical Statistics*, 4, 12–35. [3]

Rosowsky, D., and Ellingwood, B. (1992), "Reliability of Wood Systems Subjected to Stochastic Live Loads," *Wood and Fiber Science*, 24, 47–59. [1]

Smith, I., Landis, E., and Gong, M. (2003), *Fracture and Fatigue in Wood*, New York: John Wiley & Sons. [4]

Sørensen, J. D., and Svensson, S. (2005), "Reliability-Based Modeling of Moisture and Load-Duration Effects," in *Probabilistic Models in Timber Engineering, Test, Models, Applications*, ed. P. Castera, Arcachon, France: Arbora. pp. 79–86. [2]

Svensson, S. (2009), "Duration of Load Effects of Solid Wood: A Review of Methods and Models," *Wood Material Science and Engineering*, 4, 115–124. [1]

Wong, S. W., and Zidek, J. V. (2018), "Dimensional and Statistical Foundations for Accumulated Damage Models," *Wood Science and Technology*, 52, 45–65. [2,11]

Wood, L. (1951), "Relation of Strength of Wood to Duration of Stress," Report no. R1916, US Forest Products Laboratory, Madison, Wisc., USA. [1]

Zhai, Y. (2011), "Dynamic Duration of Load Models," Master's thesis, Department of Statistics, University of British Columbia, British Columbia. [1]